Finite element analysis on stress-induced birefringence of polarization-maintaining optical fiber

Rongfeng Guan (关荣锋)[1,2,3], Xueli Wang (王学立)[4] , Xuefang Wang (汪学方)[1], Dexiu Huang (黄德修)[2], and Sheng Liu (刘 胜)[1,5]

[1] *Institute of Microsystems,* [2] *Department of Opto-Electronics Engineering, Huazhong University of Science and Technology, Wuhan 430074*

[3] *Department of Applied Physics, He'nan Polytechnic University, Jiaozuo 454000*

[4] *Digital Engineering Research Center, Huazhong University of Science and Technology, Wuhan 430074*

[5] *Department of Mechanical Engineering, Wayne State University, Detroit, Michigan 48202, USA*

Received June 1, 2004

Influence of thermal-mechanical properties on the features of the panda polarization-maintaining optical fiber (PMF) in fabrication process is studied in detail by finite element method (FEM). The stress birefringence is 2.13443×10^{-4} obtained by the static analysis and 2.1269×10^{-4} by dynamic analysis. The difference in simulation by two methods is around 0.4%. The non-uniformity of stress birefringence in the fiber core is about 1.6%. Predicted results demonstrate that effect of the thermal conductive parameter on fiber thermal stress dominates. The high and uniform stress birefringence in the fiber core is obtained by appropriately selecting suitable stress region area and position.

OCIS codes: 060.0060, 060.2310, 060.2420, 060.2430.

Stress-induced polarization-maintaining optical fibers (PMF) have shown to be of importance and promising for future applications[1−4]. The PMFs of the bow-tie shape, panda shape, and ellipse cladding shape are common and these fibers must be designed by using stress birefringence principle[5]. The calculation of stress birefringence using theoretical methods is not only complex, but also difficult to obtain. In most cases, only the birefringence of the symmetry structure fiber can be calculated, or only the birefringence in fiber core can be obtained[6,7]. This is far enough from designing and fabricating high performance PMFs. The waveguide structure analytical methods, finite element method (FEM), and the corresponding commercial analysis software (such as FEMLAB), have been widely applied because of their simple calculation, practicality and high precision[8,9]. The thermal stress-induced birefringence for the panda shape fiber is analyzed by FEM in this paper. Its thermal stress distribution, the stress-induced birefringence distribution, and the relation between the stress birefringence and the stress regions are presented. The influences of different thermal parameters on the fiber stress distribution are analyzed. The simulation results are compared with the theoretical results.

As in the case of optical fibers, when the dimension of the structure in one direction (the z-direction) is very large in comparison with the other two directions (x- and y-direction) and the applied forces are assumed to act in the x-y plane and do not vary in the z-direction, the problem is assumed to be the "plane strain problem". For the plane strain problem the stress-strain relation[4] is expressed as

$$\mathbf{T} = [c]\,(\mathbf{S} - \mathbf{S}_0)\,, \tag{1}$$

where $\mathbf{T}$ is the stress vector, $\mathbf{S}$ is the strain vector, $\mathbf{S}_0$ is the initial strain vector, and $[c]$ is elasticity matrix.

The strain-displacement relation is given by

$$\mathbf{S} = \nabla_S \mathbf{u}, \tag{2}$$

where $\mathbf{u}$ is the nodal displacement tensor.

The strain energy per unit length in the direction of propagation is given by

$$F = \iint_\Omega \mathbf{S}^* \cdot \mathbf{T}\mathrm{d}x\mathrm{d}y, \tag{3}$$

where $\int\int_\Omega \mathrm{d}x\mathrm{d}y$ denotes the integration over the fiber cross section Ω. Substituting Eqs. (1) and (2) into Eq. (3), we obtain

$$F = \iint_\Omega (\nabla_S \mathbf{u})^* \cdot [c]\,(\nabla_S \mathbf{u} - \mathbf{S}_0)\,\mathrm{d}\Omega. \tag{4}$$

Dividing the fiber cross section into a number of linear triangular elements, we expand the particle displacement $\mathbf{u}$ in each element as

$$\mathbf{u} = [\mathbf{n}]^{\mathbf{T}}\,\{\mathbf{u}\}_{\mathbf{e}}\,, \tag{5}$$

where $\{\mathbf{u}\}_{\mathbf{e}}$ is the nodal displacement vectors, $[\mathbf{n}]$ is the shape function vector.

Substituting Eq. (5) into Eq. (4) and assuming that the initial strain in each element is constant, from the variational principle we obtain the following simultaneous linear equation

$$[K]\,\{\mathbf{u}\} = \{\boldsymbol{f}_T\}\,, \tag{6}$$

with

$$[K] = \sum_e \iint_e [B]\,[c]\,[B]^T\,\mathrm{d}x\mathrm{d}y, \quad \text{and} \tag{7}$$

$$\{\boldsymbol{f}_T\} = \sum_e \iint_e [B]\,[c]\mathbf{S_0}\mathrm{d}x\mathrm{d}y, \tag{8}$$

where

$$[B] = \begin{bmatrix} \{n_x\} & \{0\} & \{n_y\} \\ \{0\} & \{n_y\} & \{n_x\} \end{bmatrix}, \tag{9}$$

and $\{\boldsymbol{f}_{\boldsymbol{T}}\}$ is the global initial force vector.

Equation (8) gives the nodal displacements at all nodes of the fiber under thermal stress. Once the global particle displacement vector $\{\mathbf{u}\}$ is determined, the stress in each element is given by

$$\mathbf{T} = [c]\left([B]^T \{\mathbf{u}\}_{\mathbf{e}} - \mathbf{S}_0\right). \tag{10}$$

It is known that stress-birefringence relation satisfies stress photoelastic effect principle. It is proven that in transparent solid materials, the principal index of stress birefringence and its corresponding principal stress are coincident in the same direction, and they have relation in magnitude by the formulas[6]

$$\begin{aligned} N_x - N_y &= C\left(\sigma_x - \sigma_y\right), \\ N_y - N_z &= C\left(\sigma_y - \sigma_z\right), \\ N_z - N_x &= C\left(\sigma_z - \sigma_x\right), \end{aligned} \tag{11}$$

where N_i $(i = x, y, z)$ are the indices of the material when stress in material is not zero, σ_i $(i = x, y, z)$ are the positive stresses along x-, y-, and z-direction of the material respectively, $C = a - b$, a and b are stress-photoelastic coefficients of the material, and C is a relative stress-photoelastic coefficient of the material.

The panda PMF is an important fiber and therefore it is analyzed as a typical example in our research. Figure 1 is the geometric model of the panda fiber. The panda fiber consists of fiber core, cladding, and stress regions. The material of cladding is a pure SiO_2 layer, and the main ingredients of the core and stress areas are GeO_2/SiO_2 and B_2O_3/SiO_2, respectively. Thermal expansion coefficient of SiO_2 α_0 is $5.4\times10^{-7}/^\circ$C[7]. The doping material usually used in fiber is GeO_2, B_2O_3, or P_2O_5, the corresponding thermal expansion coefficients of them are $\alpha_{\rm Ge} = 7\times10^{-6}/^\circ$C, $\alpha_{\rm B} = 10\times10^{-6}/^\circ$C, $\alpha_{\rm P} = 14\times10^{-6}/^\circ$C[10]. Therefore, thermal expansion coefficient of a doped optical fiber can be expressed as[10]

$$\alpha = (1 - m)\alpha_0 + m\alpha_1, \tag{12}$$

where α_1 is thermal expanding coefficient of the doped material, m indicates the mole quantity of the doped material.

The parameters of fiber material to be used in modeling and simulation are Young's modulus $E = 7.8\times10^{10}$ m^2/N, Poisson's ratio $\nu = 0.186$. Thermal expansion coefficients[11] of core region a_1, cladding region a_2, and stress region a_3 are 2.215×10^{-6}, 0.54×10^{-6}, $1.45\times10^{-6}/^\circ$C, respectively. The refractive index at zero stress for core $N_{\rm core}$ is 1.4558, for cladding $N_{\rm clad}$ is 1.4478, and for stress area $N_{\rm sap}$ is 1.4418[12,13]. Photoelastic coefficients $a = -0.7572448\times10^{-12}$, $b = -4.18775\times10^{-12}$ m^2/N, related photoelastic coefficient $C = a - b = 3.4305052\times10^{-12}$ m^2/N[7].

Because the melting state of fiber cooled to room temperature is a quite complex process, the system temperature, thermal flow rate, thermal boundary condition, and the internal energy all change with time. At the same time, the corresponding material properties are also dependent on the temperature in the transmitting thermal process. For simplification, analyzed process is to assume that the system is a thermal elastic problem (no plastic deformation is generated), and the temperature field and the stress field can be decoupled and therefore can be calculated separately. We also ignore temperature dependence of material Young's modulus, Posion ratios, yield stress, and thermal expansion coefficients. Therefore, in following, we calculate stress-induced birefringence using linear static method and dynamic method, respectively.

In the static thermal stress analysis, we consider two factors that may influence the thermal stress. One factor is the difference of the thermal expansion coefficients in the fiber, the other factor is the non-uniform temperature distribution which is called temperature gradient effect. The thermal loading of the static cooling-thermal stress analysis is defined by the reference temperature and final cooling temperature, which are 1500 and 20 °C, respectively. Figures 2 and 3 show the stress distribution σ_x and σ_y in transverse cross section of the fiber individually. From Figs. 2 and 3, we know that stresses along x- and y-axis σ_x and σ_y are about $(9.8-10)\times10^{-7}$ and $(3.5-3.7)\times10^7$ $\mathrm{N/m}^2$. According to Eq. (11), we obtain the birefringence of fiber core: $B_{\rm s} = N_x - N_y = C(\sigma_x - \sigma_y) = 2.13443\times10^{-4}$. The non-uniformity of stress birefringence in the fiber core is about 1.5%. For light wave $\lambda = 1.31$ μm, its beat length $L_{\rm b} = 6.137$ mm. Figures 4 and 5 show the refractive index distribution of N_x and N_y along x- and y-axis individually. The refraction indices in the fiber core are $N_x = 1.456762$, $N_y = 1.456551$, respectively. From the figures we know that either along x- or y-axis inside the fiber core, index along x-axis is larger than

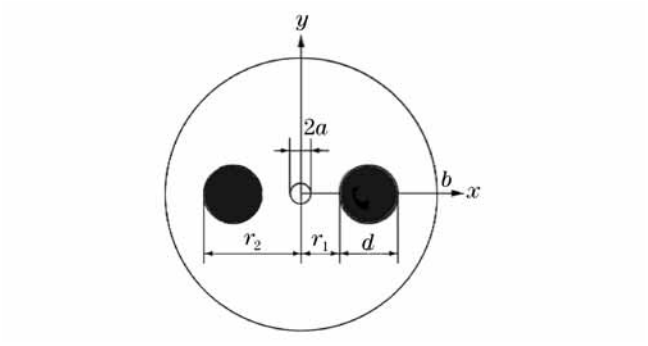

Fig. 1. Cross section structure of panda PMF.

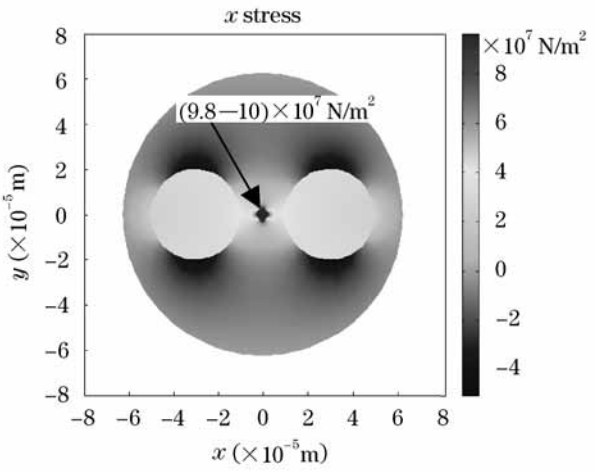

Fig. 2. Stress distributions (σ_x) of fiber cross section.

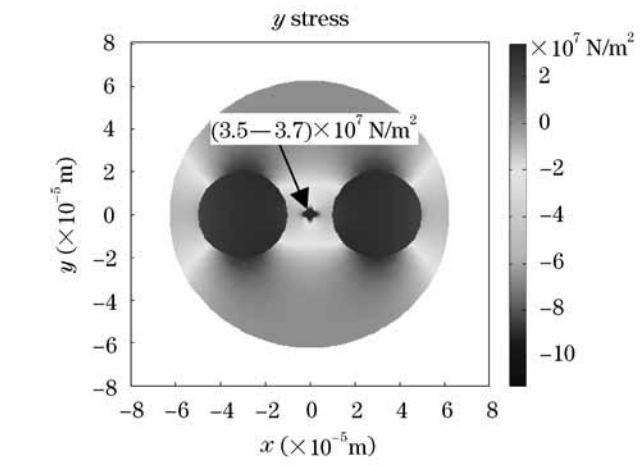

Fig. 3. Stress distributions (σ_y) of fiber cross section.

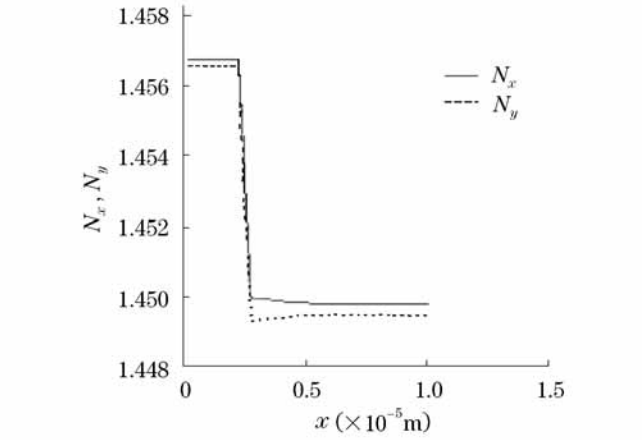

Fig. 4. N_x, N_y distributions of fiber core on x-axis.

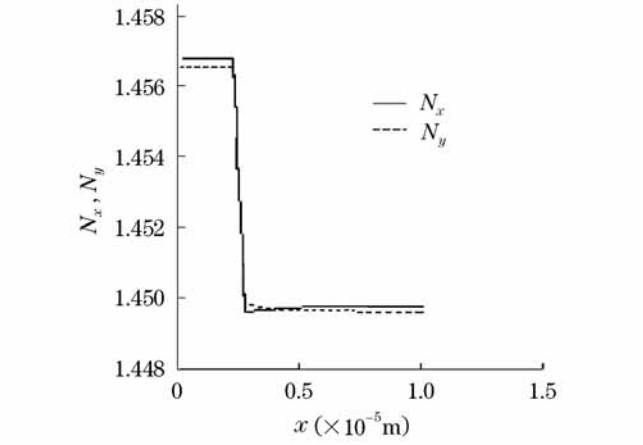

Fig. 5. N_x, N_y distributions of fiber core on y-axis.

index along y-axis. Thus the difference between N_x and N_y is birefringence, which distribution is quite uniform in fiber core. Slow axis of PMF is x-direction, and rapid axis is y-direction in the figure.

In our dynamic thermal stress analysis, we first calculate the temperature field, and then calculate thermal stress field. The geometric model of finite element analysis is the same as above. We only choose quarter of the geometric model to do analysis because of structure symmetry. Assuming thermal loads of the fiber are as following: the beginning temperature is 1500 °C and is uniformly distributed in the whole fiber, the cooling temperature is 20 °C (at room temperature). Thermal convection coefficient on boundary of the fiber is 500 W/(m^2 · °C). In analyzing thermal stress, the temperature field distribution is calculated first by heat transfer principle as state variable is applied to the model and solves the stress distribution again.

The material property parameters are used in the dynamic analysis, including the properties provided in the static analysis. Specifically, these additional properties are the fiber material mass density of 2203 kg/m^3, specific heat of 703 J/(kg · °C), thermal conductivity coefficient of 1.38 W/(m^2 · °C), and the air convection coefficient of 500 W/(m^2 · °C), etc..

Figures 6 and 7 show stress σ_x and σ_y distributions of fiber cross section in x- and y- direction after fiber cooling to room temperature. From Figs. 6 and 7 and post processing we know that stresses along x- and y-axis σ_x and σ_y are about $(9.5-10)\times10^{-7}$ N/m^2 and $(3.5-3.8)\times10^7$ N/m^2, respectively. The stress in fiber core σ_x is 9.895×10^7 N/m^2 and that of σ_y is 3.707×10^7 N/m^2. Thus, according to Eq. (11), we obtain the

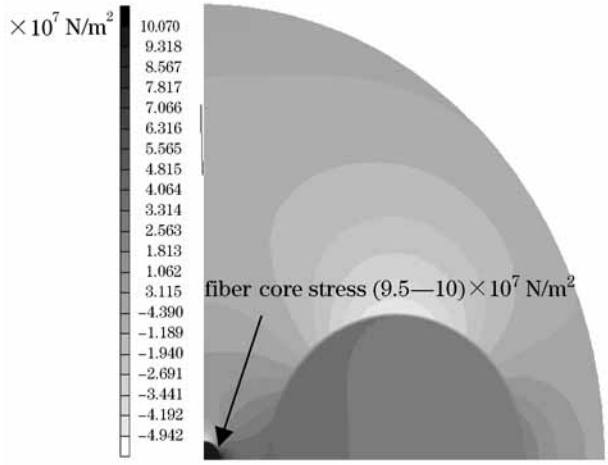

Fig. 6. Stress σ_x of fiber cross section after cooling down.

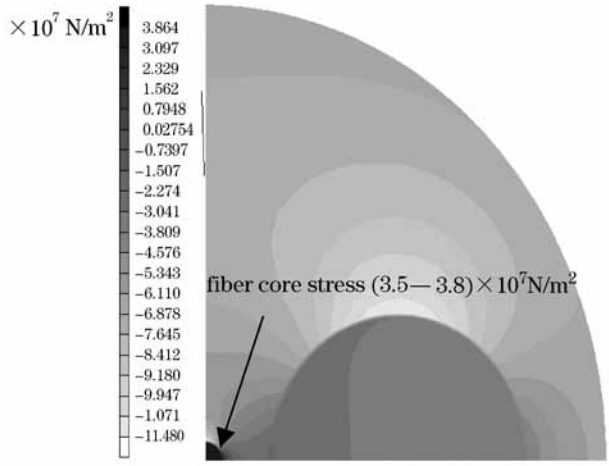

Fig. 7. Stress σ_y of fiber cross section after cooling down.

birefringence of fiber core $B = C(\sigma_x - \sigma_y) = 2.1269\times10^{-4}$. For light wave $\lambda = 1.31$ μm, the corresponding beat length $L_b = 6.25$ mm. The non-uniformity of stress birefringence in fiber core is about 1.6%.

We select different thermal convection coefficients to make parametric study for comparison. Results show that the stress distributions are basically similar. Therefore, in fabricating process of the PMF, the thermal convective coefficient has a smaller influence on the fiber stress distribution, but the thermal conductivity coefficient has a bigger influence on the fiber stress distribution. The explanation for this problem is that the outmost temperature of the fiber decreases rapidly to room temperature, thus influence of thermal convection on the stress is small; the inner thermal conduction of fiber is the main form of transmitting heat, and the influence on the stress distribution is bigger. The difference of stress birefringence simulated by the static and dynamic methods is as low as 0.4%.

Base on the thermal stress theory, the stress birefringence formulas can be derived. The formula describing the stress birefringence of panda fiber at the core center point is shown as[11]

$$B_0 = \frac{2CE\Delta\alpha\Delta T}{1-\nu}\left(\frac{d_1}{d_2}\right)^2\left[1-3\left(\frac{d_2}{b}\right)^4\right], \qquad (13)$$

where d_1 is the radius of stress region, d_2 is the distance between the panda eye center and fiber core, C is the relative stress-photoelastic coefficient of fiber, E is the Young's modulus of fiber, ν is the Poisson ratio, $\Delta\alpha$ is the difference between stress regions and cladding regions thermal expansion coefficients, $\Delta\alpha = \alpha_{sap} - \alpha_{core} = 0.91\times10^{-6}/^\circ$C, ΔT is the difference between drawing temperature and cooling temperature, $\Delta T = 1480\ ^\circ$C.

When d_1 is fixed, but d_2 changes as 22.5, 25, 27.5, 30, 32.5, 35 μm, respectively, we work out a series of birefringence values by FEM, electromagnetism field modal theory, and Eq. (13), respectively. The results are shown in Fig. 8. In the figure, the symbols "+" denote the stress birefringence B_s calculating by FEM, the solid curve denotes the stress birefringence B_0 calculating by Eq. (13), and the dotted curve denotes the modal birefringence B_m calculated by the modal theory.

Figure 8 shows that the stress birefringence calculated by both FEM and Eq. (13) agrees very well, and the result of the modal theory is slightly small. The numerical simulations demonstrate that the stress birefringence and the modal birefringence all increase with decrease of the distance d_2 between the panda eye center and the fiber core. Thus, when the radius of the panda eye is certain, larger stress birefringence will be obtained by decreasing distance between the panda eye and the fiber core, but too small distance will make the uniformity of fiber birefringence become poor.

In summary, firstly, the stress birefringence calculated by the static analysis is 2.13443×10^{-4}, and by dynamic analysis is 2.1269×10^{-4}. The stress distribution and birefringence distribution in fiber core are nearly uniform, its non-uniformity is about 1.6%. The difference of stress birefringence simulated by the static and dynamic methods is as low as 0.4%. The main thermal parameter influencing thermal stress distribution is thermal conduction in fiber, and the effect of the thermal convection between fiber and environment on the stress distribution is much smaller. Secondly, the stress birefringence of the fiber is dependent on the stress region structure, doping material, processing parameters, and fabricating environment, etc.. A larger and more uniform stress birefringence can be obtained by optimizing stress region structure, material parameters, and fabrication processing.

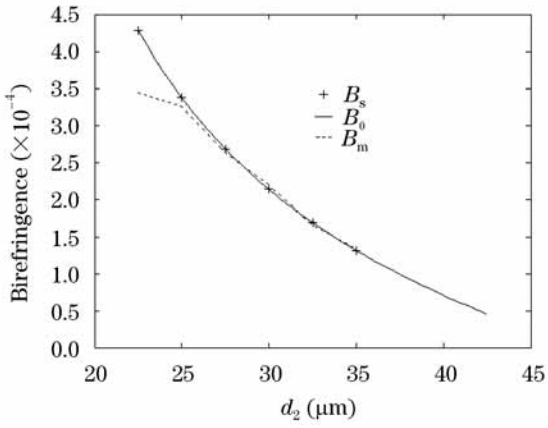

Fig. 8. The comparison of birefringence.

This work was supported by the National Basic Research Program of China under Grant No. G2000036605. R. Guan's e-mail adress is rongfengg@163.com.

References

1. Z. Meng, Y. M. Hu, S. D. Xiong, Y. Liu, M. Ni, and X. L. Zhang, Chin. J. Lasers (in Chinese) **29,** 415 (2002).
2. L. Xia, X. H. Li, Y. Z. Yin, J. Feng, J. Mao, X. F.Chen, and S. H. Xie, Acta Opt. Sin. (in Chinese) **22,** 1004 (2002).
3. S. H. Yuan, Q. Hu, and M. Q. Wang, Acta Opt. Sin. (in Chinese) **22,** 383 (2002).
4. J. Noda, K. Okamoto, and Y. Sasaki, J. Lightwave Technol. **4,** 1071 (1986).
5. Y. L. Ruan, Q. Xiang, and D. X. Huang, Chin. J. Lasers (in Chinese) **23,** 901 (1996).
6. K.-H. Tsai, K.-S. Kim, and T. F. Morse, J. Lightwave Technol. **9,** 7 (1991).
7. Y. A. Liu and B. M. A. Rahman, J. Lightwave Technol. **13,** 142 (1995).
8. C. S. Chang and H. C. Chang, J. Lightwave Technol. **15,** 1213 (1997).
9. K. Dossou, S. L. Rochelle, and M. Fontaine, J. Lightwave Technol. **20,** 1463 (2002).
10. L. Li and Y. Q. Huang, *Fundamental of Optical Fiber Communication* (in Chinese) (National Defense Industry Press, Beijing, 1992) p. 120.
11. P. L. Chu and R. A. Sammut, J. Lightwave Technol. **2,** 650 (1984).
12. Y. M. Hu, Z. Chen, Y. B. Liao, S. L. Chang, J. C. Tan and Z. Meng, Chin. J. Lasers (in Chinese) **25,** 716 (1998).
13. X. D. Zeng and Y. Y. An, Semiconductor Optoelectronics (in Chinese) **20,** 312 (1999).